ELSEVIER

Journal of Nuclear Materials 295 (2001) 83–96

journal of nuclear materials

www.elsevier.nl/locate/jnucmat

SON 68 nuclear glass alteration kinetics between pH 7 and pH 11.5

S. Gin *, J.P. Mestre

Commissariat à l'Énergie Atomique (CEA), Valrhô/Marcoule, DDRV/SCD, BP 17171, 30207 Bagnols-sur-Cèze cedex, France

Received 17 October 2000; accepted 11 January 2001

Abstract

The effect of the pH was investigated on the mechanisms of SON 68 (R7T7-type) glass alteration under 'saturation' conditions in order to delimit the pH range within which a stable, protective gel is formed. Static experiments were conducted at 90°C with an S/V ratio of 50 cm^{-1} at various imposed pH values: 7, 8, 9.5, 10, 10.5, 11 and 11.5. An additional experiment was conducted with no restriction on the pH. The kinetic study showed that a protective gel formed in all the test media, although its stability was pH-dependent: at pH 11 or higher, the precipitation of a potassium and sodium aluminosilicate led to the degradation of the gel and the lose of its protective properties. This phenomenon resulted in renewed glass alteration, leading to complete and rapid degradation of the glass into alteration products. The aluminosilicate precipitation was found to be limited by the solubility of aluminum. Below pH 10, this type of secondary phase is unlikely to precipitate and the gel should remain stable. This study, based on thermodynamic and kinetic considerations, suggests that aqueous alteration of the French SON 68 nuclear glass results in the formation of a protective gel with long-term stability between pH 7 and pH 10.

1. Introduction

This experimental study addresses two objectives: determine the pH range within which the alteration of the French SON 68 (R7T7-type) nuclear glass results in the formation of a protective gel constituting a diffusion barrier and limiting the dissolution of species from the glass; and determine the possible causes of a long-term degradation of the protective gel properties.

The pH is a key parameter in the evolution of silicates in geochemical cycles, mainly because the species H_3O^+ and OH^- take part in the hydrolysis and condensation reactions involving the covalent Si–O bond [1]. The effect of the pH on the reactivity of silicates is generally investigated through catalytic phenomena (the influence of the H_3O^+ or OH^- ion concentration in highly dilute media) as well as through the concept of equilibrium and solubility that may be shifted or modified by the pH [2,3].

From a kinetic standpoint, these mechanisms are described by a product of terms in laws describing the dissolution or precipitation of minerals or of silicate glasses [4]. Catalytic phenomena are generally included with the activation energy term in the macroscopic initial rate term, and the notion of an equilibrium between the solid and fluid is described by a chemical affinity function $f(\Delta G)$ that is related to the limiting mechanism for many authors [5].

In the simple case of a pure SiO_2 phase, the dissolution reaction can be written as follows:

$$SiO_2 + 2H_2O \leftrightarrow H_4SiO_4. \tag{1}$$

The reaction rate is expressed

$$r = k^+ a_{H^+}^n e^{-Ea/RT}\left(1 - \frac{a_{H_4SiO_4}}{K}\right), \tag{2}$$

where k^+ is the kinetic constant, n the coefficient of the pH-dependence of the reaction rate, Ea the activation energy, $a_{H_4SiO_4}$ the H_4SiO_4 activity in solution, and K the phase solubility. Increasing the solution pH, increases

* Corresponding author. Tel.: +33-4 66 79 14 65; fax: +33-4 66 79 66 20.

E-mail address: stephane.gin@cea.fr (S. Gin).

0022-3115/01/$ - see front matter
PII: S0022-3115(01)00434-2

the rate of hydrolysis of the Si–O bond and increases the solubility through dissociation of H_4SiO_4 into $H_3SiO_4^-$ and $H_2SiO_4^{2-}$ according to the following reactions:

$$H_4SiO_4 + OH^- \leftrightarrow H_3SiO_4^- + H_2O, \quad (3)$$

$$H_4SiO_4 + 2OH^- \leftrightarrow H_2SiO_4^{2-} + 2H_2O. \quad (4)$$

Recent theoretical and experimental work on nuclear glass has led the authors to question the use of such laws to describe the alteration kinetics of this type of matrix [6–12]. The primary reason for the discrepancy between the 'classic' kinetic laws based on the theoretical work by Aagaard and Helgeson [4] and the experimental data is related to the fact that the chemical affinity laws do not take into account the gel that forms between the glass and solution, and which tends to limit exchanges by diffusion between the solid and the solution, preventing a thermodynamic equilibrium from being reached between the hydrated glass and the bulk solution.

When considering the protective effect of the gel, the influence of the pH on the evolution of the alteration kinetics of a nuclear glass could thus be expected to be more complex than for the pure silica phase mentioned above – notably because of the additional link in the causality chain: the pH modifies the chemical reactions of hydrolysis and condensation of the glass species; the kinetics of the chemical reactions affect the gel structure, and thus, the diffusion coefficient of the reactive species within it.

This paper presents and discusses the results of a series of experiments in which the French SON 68 (R7T7-type) nuclear glass was altered under 'saturation' conditions at 90°C at various imposed pH values ranging from 7 to 11.5. This pH range is broader than the range expected in contact with the glass in a geological repository scenario, notably because of the buffering role of the nearfield engineered barrier.

The effect of the pH on the dissolution kinetics of SON 68 glass had previously only be described under 'initial rate' conditions [13]; this work showed in particular a double catalytic effect on the glass dissolution reaction: by H^+ or H_3O^+ ions in acidic media, and by OH^- ions in basic media. As with most aluminosilicates, the initial dissolution is minimal at near-neutral pH [14]. Under saturation conditions, the effect of the pH on the glass alteration kinetics is largely unknown. Only a few integral experiments are available in which the pH was imposed by the environmental materials (clays, cement...), but in this type of experiment it is difficult to isolate the specific effect of the pH on the glass alteration rate since the environmental materials are generally not neutral. Under saturation conditions, the pH could have the following effects:

- modify the silica saturation conditions, i.e., the apparent solubility of the glass;
- modify the protective effect of the gel, related to the pH effect on the recondensation of silicate species;
- precipitate secondary phases liable to control the glass alteration kinetics.

The possible occurrence of these phenomena was investigated by static tests at 90°C with a glass-surface-area-to-solution-volume (S/V) ratio of 50 cm^{-1} at various imposed pH values: 7, 8, 9.5, 10, 10.5, 11 and 11.5 (the equilibrium pH of SON 68 glass at this S/V ratio and temperature is 9.1). An additional control experiment was conducted with no restriction on the pH. The 50 cm^{-1} S/V ratio was selected to ensure that Si 'saturation' conditions favorable to the development of protective gels were quickly reached.

2. Experimental protocol

2.1. Introduction

The static tests were designed to observe the glass alteration kinetics by analysis of solution samples taken at various intervals over a 20-month period. The reactors were 120 ml Savillex PTFE containers in which SON 68 glass powder (4.65 g of 63–100 μm size fraction) was placed in contact with 80 ml of ultrapure water. Eight tests were conducted at a constant temperature of 90°C: seven tests at imposed pH values of 7, 8, 9.5, 10, 10.5, 11 and 11.5, and one with unrestricted pH. The experimental conditions are summarized in Table 1.

2.2. Glass specimen preparation

The test glass was the French SON 68 inactive reference glass (composition: Table 2). The 63–100 μm size fraction was obtained by milling and sieving glass fragments obtained after crushing sample rods with a hammer. The powder was cleaned ultrasonically in acetone, then in alcohol, and finally in ultrapure water, The specific surface area as determined by the BET method using Kr was 860 ± 40 cm^2 g^{-1}.

Table 1
Characteristics of imposed-pH solubility tests

Parameter	Value
Mode	Static
Temperature	90°C
S/V ratio	50 cm^{-1}
Solution volume	80 ml
Glass	SON 68 (inactive reference glass)
Powder mass	4.651 g
pH	Imposed: 7, 8, 9.5, 10, 10.5, 11 and 11.5 +1 test at unrestricted pH
pH adjustment	Manual
Duration	20 months
Elements analyzed	Si, B, Na, Al, Ca, Li, Mo

Table 2
SON 68 (R7T7-type) glass composition

Oxide	wt%	Element	wt%	Oxide	wt%	Element	wt%
SiO_2	45.48	Si	21.26	Y_2O_3	0.20	Y	0.16
Al_2O_3	4.91	Al	2.60	MoO_3	1.70	Mo	1.13
B_2O_3	14.02	B	4.35	MnO_2	0.72	Mn	0.46
Na_2O	9.86	Na	7.31	CoO	0.12	Co	0.09
CaO	4.04	Ca	2.89	Ag_2O	0.03	Ag	0.03
Li_2O	1.98	Li	0.92	CdO	0.03	Cd	0.03
ZnO	2.50	Zn	2.01	SnO_2	0.02	Sn	0.02
ZrO_2	2.65	Zr	1.96	Sb_2O_3	0.01	Sb	0.01
Fe_2O_3	2.91	Fe	2.04	TeO_2	0.23	Te	0.18
NiO	0.74	Ni	0.58	Cs_2O	1.42	Cs	1.34
Cr_2O_3	0.51	Cr	0.35	BaO	0.60	Ba	0.54
P_2O_5	0.28	P	0.22	La_2O_3	0.90	La	0.77
UO_2	0.52	U	0.46	Ce_2O_3	0.93	Ce	0.79
ThO_2	0.33	Th	0.29	Pr_2O_3	0.44	Pr	1.36
SrO	0.33	Sr	0.28	Nd_2O_3	1.59	Nd	1.36
						O	45.21

2.3. Test procedure

The leaching solutions consisted of ultrapure water with KOH and HCl titrating solutions prepared from Normapur products. The pH was adjusted at 90°C and verified before initiating the test. The test starting point was the moment the powder was introduced into the reactor, which included a magnetic stirring rod and was placed on a stirring device inside an oven regulated at 90°C ± 2°C.

The pH was checked periodically and adjusted to the setpoint value if outside the following tolerance limits:

- pH 7: 6.5–7.5
- pH 8: 7.7–8.5
- pH 9.5: 9.3 – 9.7
- pH 10: 9.8 – 10.2
- pH 11: 10.8 – 11.2
- pH 11.5: 10.8 – 11.7

Note. The amplitude of the acceptable variation range depended on the setpoint pH value (it is increasingly difficult to stabilize the pH as the value moves away from the glass equilibrium pH).

Solution samples were taken at the following intervals: 1, 14, 28, 56, 97, 152, 240, 372 and 594 days. Each 1 ml sample was ultrafiltered to 10,000 dal. (cutoff threshold: approx. 2 nm), then, diluted in two volumes of 1N HNO_3. ICP-AES analysis was used to determine Si, B, Na, Al, Ca, Li and Mo with an uncertainty range of 3–5% depending on the elements.

2.4. Expression of results

The *altered glass percentage* was determined at each sampling interval from the following relation

$$\%G_a = 10^{-1}\frac{C_B V}{m_0 X_B}, \tag{5}$$

where C_B is the boron concentration (mg l^{-1}) in solution, V is the solution volume (l), m_0 is the initial glass powder mass (g) and X_B is the boron mass fraction in the glass. Boron is an good alteration tracer for this type of glass, as it is primarily a network former and is not retained in the alteration products [15].

The *normalized mass loss* was calculated from the following relation:

$$NL_i = \frac{C_i}{X_i(S/V)}, \tag{6}$$

where C_i is the concentration (mg l^{-1}) of element i in solution, S/V is the ratio (m^{-1}) between the glass surface area and the solution volume, and X_i is the mass fraction of element i in the glass. NL_i, expressed in g m^{-2}, is used to assess the quantity of altered glass when calculated for the mobile elements (B, Na), and to determine the retention capability of the alteration products for the less mobile elements (notably Si). In the case of a highly altered glass specimen, the grain size reduction is taken into account by means of the shrinking-core model described by Jégou [12].

The *retention factor of element i in the glass alteration products* is defined by comparison with boron (the glass alteration tracer) in the following relation:

$$f_i = 1 - \frac{NL_i}{NL_B}. \tag{7}$$

The *glass alteration rate* is defined as follows:

$$r = \frac{d(NL_B)}{dt}, \tag{8}$$

where r is expressed in g m^{-2} d^{-1} and NL_B in g m^{-2}. The maximum glass alteration rate observed in dilute media is termed the *initial rate*, designated r_0. The initial rate

characterizes the glass resistance to hydrolysis, and depends only on the temperature and pH [13].

2.5. Characterization of the altered glass samples

SEM observations (JEOL JSM6330F, 15 kV, EDS analysis with PGT system) were performed on samples altered for 240 days at pH 11.5. We performed direct observations of the altered grain surface to reveal the presence of crystallized phases at the interface gel/solution, and also observations of cross-sections through altered glass powder (grains were embedded in Araldite AY130 resin and wet-polished with SiC paper) in order to study the chemical composition of the gel.

The altered glass powder was also characterized by X-ray diffraction (Seifert XRD 3000 diffractometer + scintillation counter, Cu cathode with Bragg–Brentano detection geometry).

3. Results

3.1. pH Variation

Fig. 1(a) shows the evolution of the pH (measured at 90°C) in the experiment at pH 7. Note the very frequent pH corrections required during the first three months of the experiment to maintain the pH within the setpoint range (6.5–7.5); during the first days, the pH occasionally even exceeded 8. After the first 100 days, the pH varied slowly, and the corrections were therefore, less frequently necessary. Expressed in terms of H^+ ion consumption during glass alteration (Fig. 1(b)), the pH variation shows two characteristic phases: the proton consumption increased very rapidly from 0 to 40 days, then leveled off. This phenomenon is discussed below in relation with glass dissolution, and notably with the interdiffusion of protons and alkali metal cations from the glass.

Fig. 2(a) shows the evolution of the pH (measured at 90°C) in the experiment at pH 8. The H^+ ion consumption was about 100 times lower than at pH 7 (Fig. 2(b)); otherwise, the curves obtained at pH 8 are similar in shape to the results at pH 7.

No pH adjustment was necessary during the experiments at pH 9.5, 10 and 10.5. During the tests at pH 11 and pH 11.5, the pH remained at the setpoint value for about 100 days (pH 11) or 56 days (pH 11.5) before slowly diminishing to 10.8; the pH values were not corrected during either of these tests.

3.2. Glass alteration

3.2.1. Altered glass fraction after 1 day and after 594 days

Fig. 3 shows the altered glass fractions after 1 day and after 594 days for all eight experiments. Under conditions far from saturation (after 1 day), the altered glass quantity was relatively independent of the pH in the range from pH 7 to pH 10, and corresponded to an altered glass thickness of about 20 nm.

Note. The alteration measured after 1 day does not correspond to initial rate conditions indicated in Table 3. Depending on the pH, the mean alteration rates between 0 and 1 day ranged from $r_0/20$ to $r_0/100$.

Over the longer term (594 days), the altered glass fraction was highly pH-dependent. The minimum alteration was observed at pH 9.5. The alteration increased sharply above and below the minimum value, with significantly greater pH-dependence in highly basic media than in neutral or slightly basic media. The glass specimen was almost totally altered after 240 days at pH 11.5.

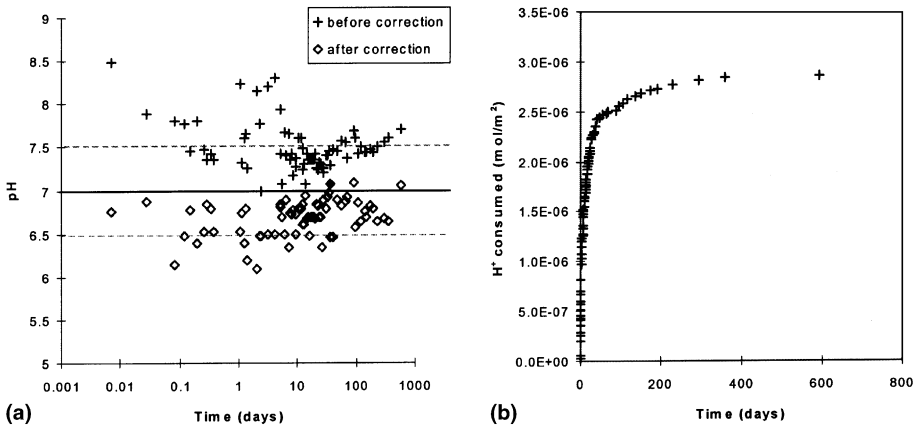

Fig. 1. (a) pH versus time in experiment at imposed pH 7; (b) H^+ ion consumption by the glass dissolution reaction, estimated from 10^{-1} N HCl make up volume.

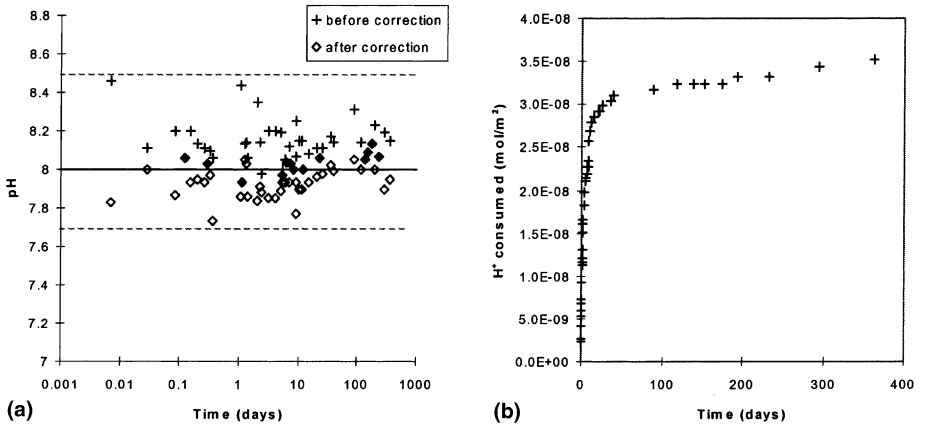

Fig. 2. (a) pH versus time in experiment at imposed pH 8; (b) H^+ ion consumption by the glass dissolution reaction, estimated from 10^{-1} N HCl make up volume.

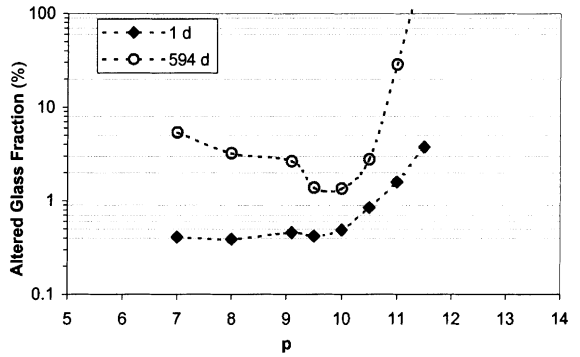

Fig. 3. Altered glass fractions after 1 day and after 594 days versus imposed leaching solution pH.

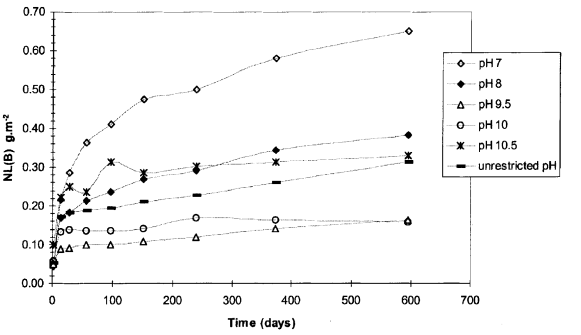

Fig. 4. Normalized glass mass loss versus time calculated from boron release for tests at pH 7 to pH 10.5.

Table 3
Initial dissolution rate of SON 68 glass versus pH at 90°C (from Advocat [16])

pH	r_0(g m^{-2} d^{-1})
7	0.9
8	1.8
9.1	4.7
9.5	5.0
10	10.4
10.5	16.4
11	24.1
11.5	42.0

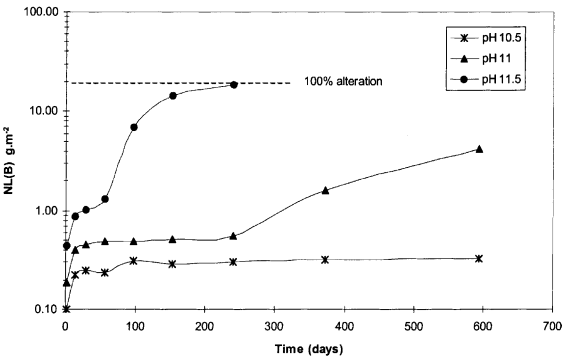

Fig. 5. Normalized glass mass loss versus time calculated from boron release for tests at pH 10.5, 11 and 11.5. (Note logarithmic scale on *Y*-axis, unlike Fig. 4.)

3.2.2. Normalized boron mass loss

The normalized glass mass losses calculated from the boron release are shown in Fig. 4 for the tests conducted at pH 7 to 10.5. In each case, the normalized mass losses increased rapidly during the first few weeks and more slowly thereafter.

Fig. 5 shows the normalized glass mass losses calculated from the boron release for the tests at pH 10.5, 11 and 11.5. At pH 11.5 the alteration rate diminished sharply between 10 and 50 days, followed by renewed

alteration until practically all the grains were transformed into alteration products. The same phenomenon was observed at pH 11, although the renewed alteration occurred much later than at pH 11.5. No such renewed alteration occurred at pH 10.5. The mechanism involved in this phenomena must be identified in order to consider the possibility of such behavior at pH values more representative of actual repository conditions.

3.3. Alteration rate

The variation of the glass alteration rate over time in the test media is shown in two ways. The rates are indicated in g m^{-2} d^{-1} versus time between 0 and 594 days (Fig. 6), then compared in Fig. 7 with the initial rate r_0, which depends on the pH according to a relation of the type $r_{0(\mathrm{pHx})} = r_{0(\mathrm{pH7})} \times 10^{0.39(x-7)}$ where $x > 7$ [16]. The initial rate was calculated for each test at the setpoint pH (Table 3). The r/r_0 ratio reflects the drop in the glass alteration rate from the maximum rate in each test.

Fig. 6 shows a rapid drop in the glass alteration rate that is relatively pH-independent in the range between pH 9 and pH 10.5, with a slower drop in the rate at pH 7–8, as well as at pH 10.5 and 11. The alteration kinetics were radically different above pH 11. A final rate on the order of 10^{-4} g m^{-2} d^{-1} was reached after 250 days at pH values up to 10.5. The existence and consequences of a residual alteration rate on the long-term behavior of nuclear glass is a major issue that will be addressed in future work.

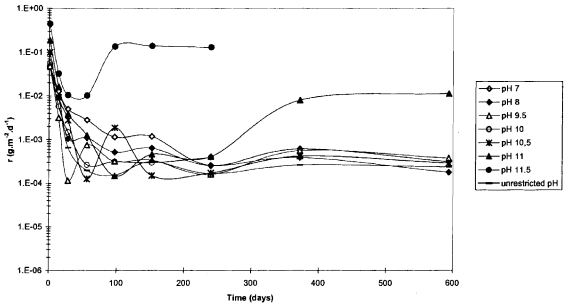

Fig. 6. Glass alteration rate versus time in various media at imposed pH. The accuracy of the rate below 10^{-3}g m^{-2} d^{-1} is poor and the fluctuations are not significant. Note that below pH 11 the final rates are relatively independent of the pH.

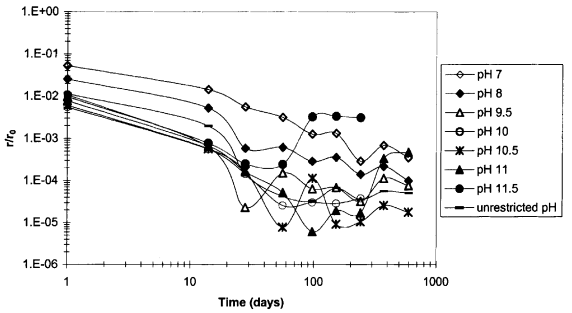

Fig. 7. Evolution of the ratio between the alteration rate (r) and the initial rate (r_0). The precision on the r/r_0 ratio below 10^{-4} is poor and the fluctuations are not significant.

Considering that the initial rate is highly pH-dependent (Table 3), it is also of interest to discuss the drop in the glass alteration rate compared with the initial rate. Fig. 7 illustrates a number of points:

- In the pH range from 9 to 11, the alteration rate dropped by over four orders of magnitude from the initial rate r_0 within about one month.
- The uncertainty on the rate calculation was too great for values below $10^{-4}r_0$ to attribute the fluctuations in the r/r_0 ratio to a particular mechanism.
- At pH values above the glass equilibrium pH (9.1), the rate drop was pH-independent, at least until renewed alteration occurred at the very basic pH values.
- Below the glass equilibrium pH, the importance of the rate drop diminished with the pH.
- Renewed alteration at pH 11 and 11.5 caused the glass alteration rate to increase by a factor of 20 compared with the rate under saturation conditions.

3.4. Dissolved silicon concentration

The silicon concentrations measured by ICP-AES in solutions filtered to 10 000 dal. are shown in Fig. 8, which highlights the following points:

- The Si concentrations were identical at pH 7, 8 and 9.5.
- The Si concentrations were slightly higher with unrestricted pH than at pH 9.5, even though the free pH was below 9.5.

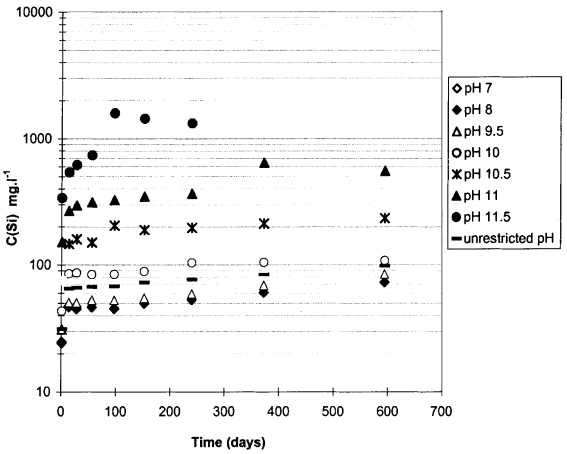

Fig. 8. Silicon concentration in the leachate versus time during 7 tests at imposed pH and one test at unrestricted pH. The data points at pH 7 and pH 8 coincided.

- The Si concentrations increased sharply with the pH above 9.5.
- The rate calculated from silicon diminished significantly over time but never ceased entirely.
- The renewal of alteration at pH 11 and 11.5 resulted in a sharp rise in the silica solubility.

At neutral or slightly basic pH values, the stable silica form is H_4SiO_4. As the pH rises, this species dissociates into $H_3SiO_4^-$ and $H_2SiO_4^{2-}$ anions according to the following reactions:

$$H_4SiO_4 \leftrightarrow H_3SiO_4^- + H^+ \qquad (K_1), \tag{9}$$

$$H_3SiO_4^- \leftrightarrow H_2SiO_4^{2-} + H^+ \qquad (K_2), \tag{10}$$

where $K_1 = 10^{-9.17}$ and $K_2 = 10^{-10.17}$ at 90°C [17].

If the glass could be considered as a form of pure silica, glass dissolution could be expressed simply as follows:

$$(SiO_2)_{glass} + H_2O \rightarrow H_2SiO_4. \tag{11}$$

The glass solubility would be equal to the H_4SiO_4 concentration at saturation. This hypothesis constituted the basis for developing the first-order kinetic model:

$$r = r_0\left(1 - \frac{C_{H_4SiO_4}}{C^{sat}_{H_4SiO_4}}\right) = r_0\left(1 - \frac{C_{Si}}{C^{sat}_{Si}}\right), \tag{12}$$

where $C^{sat}_{H_4SiO_4}$ corresponds to the glass solubility [18]. $C^{sat}_{H_4SiO_4}$, unlike C^{sat}_{Si}, is not pH-dependent. Eqs. (9) and (10) can be used to establish the relation between the dissolved silicon concentration and the pH:

$$C_{Si} = C_{H_4SiO_4}\left(1 + \frac{K_1}{10^{-pH}} + \frac{K_2}{10^{-2pH}}\right). \tag{13}$$

The H_4SiO_4 concentration was calculated from Eq. (13) for all the tests. The variations over time of the logarithm of the H_4SiO_4 concentration between 1 and 594 days are plotted in Fig. 9 for all the tests. The H_4SiO_4 concentrations were not identical in all the tests, although the should be if $C^{sat}_{H_4SiO_4}$ corresponded to the glass solubility. At pH values above 9.5, the H_4SiO_4 concentration tended to increase in time, even though the glass alteration rate dropped by over four orders of magnitude from the initial rate r_0 (Fig. 9). This result indicates that from a kinetic standpoint the glass cannot be considered as a form of pure silica, and that Eqs. (11) and (12) are not suitable for modeling glass alteration.

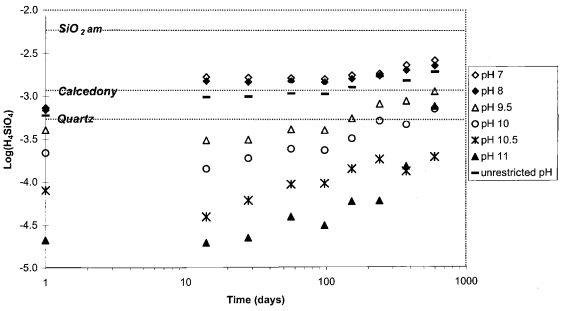

Fig. 9. H_4SiO_4 concentration in the leachate versus time. The calculation assumes the coexistence of only the following species: H_4SiO_4, $H_3SiO_4^-$ and $H_2SiO_4^{2-}$. The solubility limits of three pure silica phases are indicated in broken lines.

The retention factors of Si in the glass alteration products, f_{Si}, calculated from Eq. (7) are pH and time dependent. Generally they increase until 28 days and remain almost constant after. The values f_{Si} are close to 0.9 at pH 7 (i.e. 90% of the hydrolyzed Si remains in the gel) and decrease with pH in the range [pH 7; pH 10] until 0.45. Above pH 10, f_{Si} are not pH-dependent as long as the gel remains protective.

3.5. Renewed alteration at pH 11 and 11.5

3.5.1. SEM and XRD characterization of the alteration products

Renewed alteration was observed at pH 11.5 about 50 days into the experiment (Fig. 5). Direct SEM observation of the altered grain surface (Fig. 10) revealed the presence of two types of crystallized phases: honeycomb structures characteristic of phyllosilicates [19] and radiating acicular crystals (the latter were not observed at lower pH values).

SEM observations of cross-sections through altered glass powder grains (Figs. 11 and 12) reveal a peripheral layer about 6 μm thick consisting mainly of acicular crystals, and an inner layer ranging from 5 to 30 μm thick with no specific structural features. The phyllosilicates are not visible on the cross-sections. The pristine core is clearly visible in the grains observed along their major diameter. The EDS element maps of these grains (Fig. 13) indicate the presence of Na in the core region, confirming that the glass was unaltered. The aluminum distribution was very heterogeneous, with higher concentrations in the outer layer.

The outer crystal-rich layer and the inner alteration layer were submitted to a more detailed SEM examination on the cross-sections (Fig. 12); the EDS map for this region (Fig. 14) shows the following features:

- the acicular crystals consisted of Si, Al, K and Na;
- the inner alteration film was highly depleted in Al (a phenomenon that had never been observed before);
- potassium from the KOH solution used to adjust the pH to 11.5 was present in the alteration film, but also in large quantities in the external crystals;
- iron and, to a lesser extent, zinc were concentrated in a thin film between the acicular crystals and the alteration film, this could well be the phyllosilicate layer (Fig. 10).
- Zr and the rare earth elements were found in the gel.

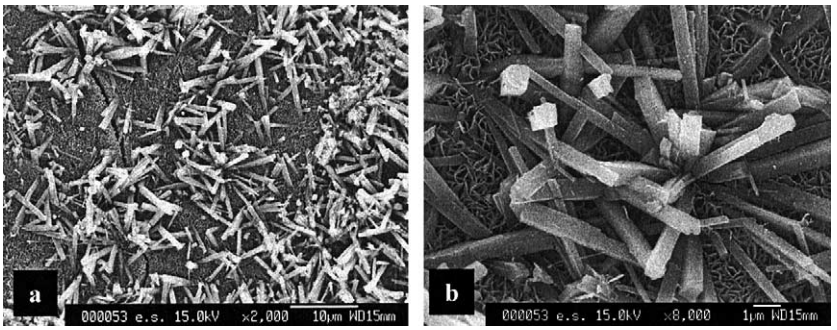

Fig. 10. (a) SEM image of the surface of glass grains altered at pH 11.5; (b) 4× enlargement of Fig. 10 (a) (the honeycomb structure beneath the acicular crystals is characteristic of the phyllosilicates).

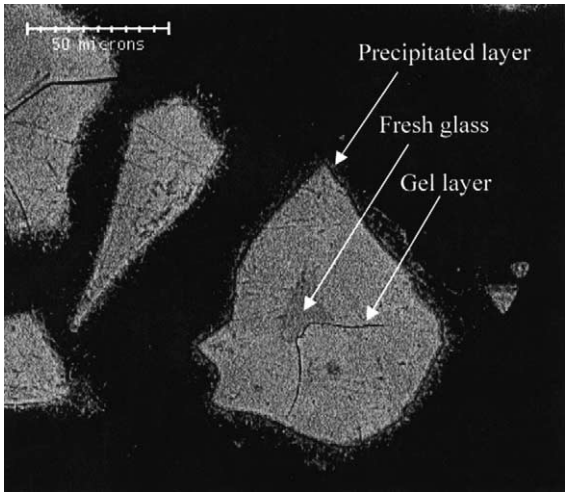

Fig. 11. SEM image of a cross-section through a glass grain altered at pH 11.5.

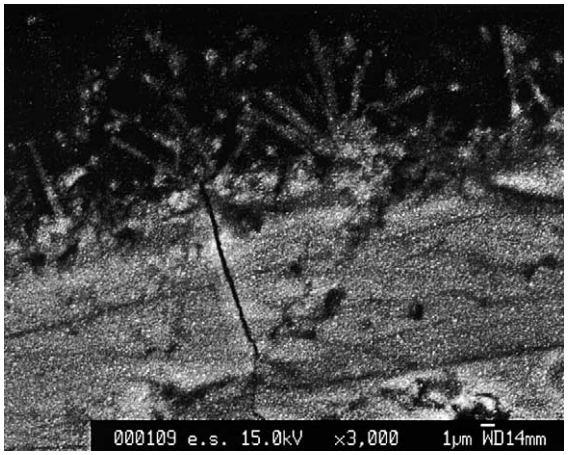

Fig. 12. SEM image of a cross-section through the outer portion of a glass grain altered at pH 11.5, showing the acicular crystals and the underlying gel layer.

Glass powder grains altered at other pH values were also observed directly. Only the grains altered at pH 11 and 11.5 developed external acicular crystals consisting of Si, Al, K and Na; only phyllosilicates were observed on the other grains.

The glass powder altered at pH 11.5 was also characterized by XRD. A single-phase was clearly observed (Fig. 15): a potassium aluminosilicate $K_2Al_2Si_4O_{12}$,-xH_2O (JCPDS file 16–692). The characteristic phyllosilicate phase was not detected, either because of its limited crystallinity or its limited abundance. This finding is consistent with the SEM chemical analysis results. The substitution of Na for K in this phase has no significant effect on the mesh parameters, suggesting that the precipitated phase could consist of $(K, Na)_2Al_2$-Si_4O_{12}, xH_2O. This phase will be designated $Alc_2Al_2Si_4O_{12}$ in the remainder of this study.

3.5.2. Behavior of dissolved species

The renewed alteration observed during the experiment at pH 11.5 was accompanied by a sudden drop in the dissolved Al concentration and a major increase in the dissolved silicon concentration although the dissolved silicon flow remained well below that of the alteration tracers (B, Na, Li). This resulted in greater silicon retention in the alteration products. It is not impossible that a fraction of the silicon was present in colloidal form, but as all the solutions were analyzed after ultrafiltration to 10 000 dal., no data are available to confirm this.

The dimensions of the $Alc_2Al_2Si_4O_{12}$ crystal can be estimated from Figs. 10–13 at approximately $5 \times 0.7 \times 0.7$ μm^3 (i.e. 2.45 μm^3) with some 20 vol.% crystals in the outer layer. Assuming a crystal density of 2.5 g cm^{-3} by analogy with other aluminosilicates, and based on an aluminum mass fraction of 12% in the crystal, the quantity of aluminum contained in these phases is about 120 mg. This value corresponds to the total amount of Al initially available in the glass; it is also 50 times greater than the dissolved Al concentration

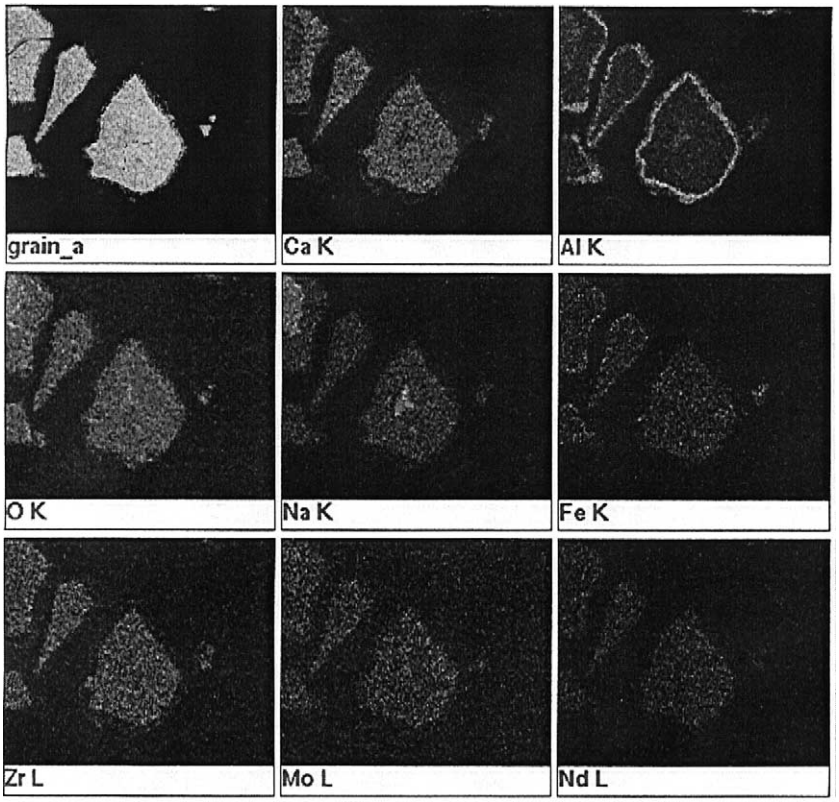

Fig. 13. EDS map of the zone corresponding to Fig. 11 (SON 68 glass grains altered in a solution at pH 11.5.

in solution when the alteration resumed. The aluminium in the $Alc_2Al_2Si_4O_{12}$ crystals, therefore does not come mainly from the solution. In view of the Al depletion of the gel, as shown by the EDS maps, it is reasonable to conclude that the gel is the primary source of aluminum for the $Alc_2Al_2Si_4O_{12}$ phase. The precipitation of the $Alc_2Al_2Si_4O_{12}$ phase can thus be related to the renewal of glass alteration.

4. Discussion

4.1. Overview

The results show that the minimum glass alteration occurred at pH 9.5, a value slightly higher than the glass equilibrium pH (9.1 under these conditions). The pH corrections performed for the tests at pH 7 and 8 and the pH variations measured during the tests at pH 11 and 11.5 show that the pH slowly tends toward the equilibrium value. After 594 days of static-mode alteration at 90°C and 50 cm^{-1}, the minimum alteration obtained at pH 9.5 corresponded to an altered glass thickness of 65 nm. This thickness is equivalent to the alteration measured on the same glass at higher S/V ratios (200 cm^{-2} [16]; 2000 cm^{-1} [20]).

The observed decrease in the alteration rate was independent of the pH for values ranging from 9.5 to 11.5 (until renewed alteration occurred). Below the glass equilibrium pH, however, the rate reduction was less significant at lower pH values.

Quasi steady-state dissolved silicon concentrations were reached in a few days for the tests conducted at pH values below 10.5. In more basic media, the silicon concentrations increased significantly with the pH and continued to do so appreciably over time. Strictly speaking, regardless of the pH, saturation of the solution with respect to silicon (indicating a solubility limit) was not observed within the experimental time frame. The following discussion will refer to 'quasi steady-state' conditions or 'apparent solubility' with regard to this aspect of silicon behavior.

Renewed glass alteration was observed after 50 days at pH 11.5 and after 250 days at pH 11. SEM and XRD examinations revealed the presence of an alkali metal aluminosilicate, the precipitation of which may be related to the renewal of glass alteration. The effect of the pH on the gel formation mechanisms and on its protective properties are discussed below, as are the

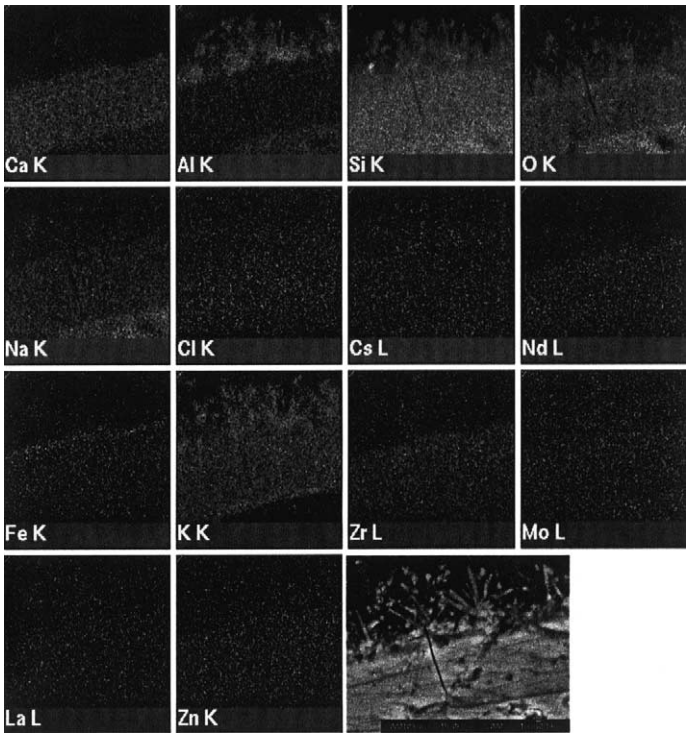

Fig. 14. EDS elemental map of the outer portion of a glass grain altered at pH 11.5.

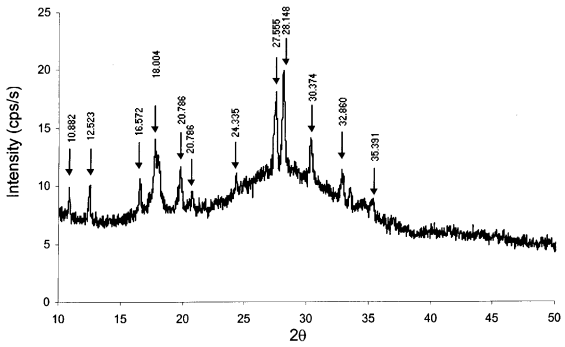

Fig. 15. XRD diagrams of SON 68 glass powder altered at pH 11.5. All the identified peaks correspond to the $K_2Al_2SiO_4, xH_2O$ phase (JCPDS file 16-692).

occurrence and effects of the precipitation of secondary phases.

4.2. Importance of interdiffusion

The interdiffusion mechanism leads to preferential release of the alkali metal ions associated with non-bridging oxygen atoms in the glass [21,22]. Although this mechanism is known to predominate during the initial stages of glass alteration, its role at advanced stages of reaction progress remains uncertain.

In all the tests at pH values ranging from 7 to 10.5, lithium was released at a higher rate than boron: this phenomenon could be characteristic of interdiffusion. Conversely, sodium was found to be less mobile than lithium, and sometimes less mobile than boron; the sodium appears to be retained in the gels and alteration products. Assuming the dissolved boron corresponds to the hydrolysis front and the lithium to the interdiffusion front, the thickness of the ion exchange region can be shown to increase in time. At pH 7, for example, the ion exchange region grew from 6.5 nm after 7 days to 65 nm after 594 days. This result could be interpreted by postulating that interdiffusion – in fact, the diffusion of molecular water in the pristine glass – could be reason for a residual alteration rate. This explanation, which is consistent with the interpretation proposed by Grambow [23], will remain a simple hypothesis as long as a clear correlation cannot be demonstrated for various glass compositions between the residual rate and the water diffusion coefficient within the glass structure.

4.3. Apparent glass silica solubility

The term 'apparent solubility' is subject to various interpretations, and must be clarified here before pur-

suing the discussion. Quasi steady-state silicon concentrations are generally observed after a few days or weeks during glass alteration tests. These quasi steady-state conditions result from the competition between the hydrolysis flow and the condensation flow responsible for the formation of the gel. Because these mechanisms depend to a large extent on the characteristics of the external environment, we use the term 'apparent glass solubility' to designate the quasi steady-state conditions reached by the system (glass–gel-solution-external medium).

Assuming the quasi steady-state silicon concentrations measures after 100 days of alteration correspond to the apparent glass solubility at that point in time, we compared the experimental data with the true solubility curves of two silica polymorphs: amorphous silica and chalcedony (Fig. 16).

SON 68 glass has in the past been compared with chalcedony, mainly because the apparent solubility of the glass at unrestricted pH is close to the true solubility of chalcedony. The present study shows that the glass behavior is quite different from that of a pure silica phase. While the apparent solubility of the glass varies little between pH 7 and pH 9 (as is also the case with pure silica), it increases much less with the pH than does the solubility of chalcedony or of amorphous silica (Fig. 16).

The fact that the apparent solubility increases more slowly with the pH for SON 68 glass than for chalcedony or for amorphous silica is the evidence of the effect of the gel-forming elements other than silicon (Al, Ca, Zr, REE, etc.). Studies of the kinetically limiting role of these elements [6,24] have demonstrated that their presence in the glass contributes to the formation of more protective gels and tends to diminish the apparent glass solubility.

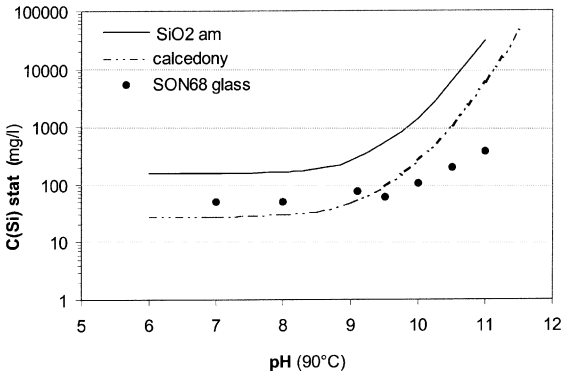

Fig. 16. Apparent glass silicon solubility versus pH, compared with true solubility of pure silica phases. For SON 68 glass, the indicated values are dependent not only on the temperature but also on the ability of the medium to supply or remove silica. This dependence on the medium distinguishes the apparent solubility from the true solubility.

4.4. Relation between glass alteration kinetics and silicon behavior

Silicon has generally been considered the kinetically limiting element [18,25]; most of the kinetic laws thus established, direct relations between boron (alteration tracer) and silicon. However, recent studies [11,12] have shown that this relation is not so direct. The results of the present study shed new light on this issue.

Fig. 17 reveals a linear relation between the quantity of altered glass $NL(\mathrm{B})$ and the dissolved silicon concentration at pH values ranging from 9.5 to 11.5:

$$NL(\mathrm{B}) = 1.6 \times 10^{-3} C_{\mathrm{Si}} \quad r^2 = 0.990. \tag{14}$$

Outside this pH range, the relation between $NL(\mathrm{B})$ and C_{Si} is no longer linear. At pH 7 and pH 8 the altered glass quantity increases although the Si concentration remains constant. Intermediate behavior is observed at pH 9.1 (corresponding to the experiment at unrestricted pH).

The relation between the quantity of altered glass and the dissolved silicon concentration can be interpreted in two ways: it may be assumed that the increasing apparent solubility of the glass with the pH is responsible for the increased glass alteration or, on the contrary, that the silicon concentration increases because the glass is altered to a greater extent at very basic pH values (in which case the silicon concentration is the consequence of the altered glass quantity).

The only driving force behind glass dissolution was long considered to be the difference in the silicon concentration (between the saturation value and the instantaneous value at time t) at the glass/gel interface. The French LIXIVER model is based on this hypothesis, arising from theoretical considerations proposed by

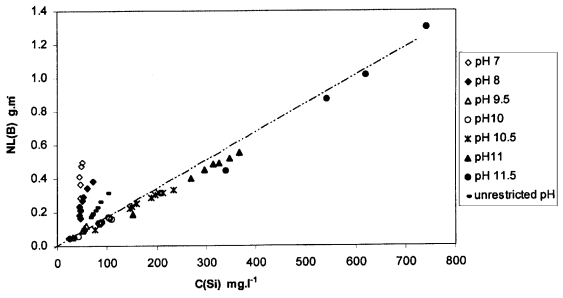

Fig. 17. Altered glass quantity $NL(B)$ versus dissolved silica concentration in tests at imposed and free pH. The data are plotted up to 200 days at pH 11 and 56 days at pH 11.5. The subsequent renewal of alteration in both cases reflects a radical change in the limiting mechanism.

Grambow [18] in 1985. Recent findings suggest the existence of several driving forces for glass dissolution [11]. It has been established that the difference between the true solubility associated with the chemical potential of the glass and the dissolved silicon concentration constitutes a powerful and permanent driving force glass. Jégou [6] showed that when a pristine glass sample was placed in a solution apparently saturated with Si, it was altered until a protective gel formed. The failure to reach the true solubility is attributable to the reverse reaction of gel formation and secondary phase precipitation. We have also established that the nonprotective gel formed during the initial-rate phase also constitutes an other driving force [11]. This can be explained by the fact that the nonprotective gel develops a large specific surface area, and exhibits a strong silicon sorption capacity. Saturation of some or all of the gel is a prerequisite to the formation of a protective gel. Inasmuch as the initial glass dissolution rate increases rapidly with the pH, the quantity of non-protective gel formed under initial-rate conditions also increases significantly with the pH. This explains why the quantity of glass that must be dissolved to saturate the gel is pH-dependent. When the nonprotective gel becomes saturated with respect to Si, the gel becomes protective (i.e., constitutes a significant diffusion barrier) and a quasi steady-state Si concentration is established as the hydrolysis and condensation flows tend to balance. The quasi steady-state concentration does not represent a thermodynamic equilibrium between the glass and solution; it corresponds to a dynamic steady-state – the difference in the chemical potential between the glass and the bulk solution, which constitutes the permanent glass dissolution motor, is offset by the diffusion barrier effect of the gel.

We noted that between pH 9.5 and pH 11.5 the decrease in the glass dissolution rate was independent of the pH (Fig. 7). In view of the preceding discussion, this implies that the gels formed between pH 9.5 and pH 11.5 exhibit the same protective properties. We also noted that the silicon fraction retained in the gel was independent of the pH 9.5 and pH 11.5. The recondensed silicon fraction is, thus, independent of the pH within this range. It is, therefore, reasonable to assume that the dissolved silicon concentration – i.e., the difference between the hydrolyzed quantity and the recondensed quantity – is proportional to that dissolved glass mass. A major conclusion can, thus, be formulated at this point: at pH values exceeding 9.5 and in the absence of precipitation resulting in degradation of the gel, the gel exhibits protective properties independent of the pH.

The conclusions reached in the pH range between 9.5 and 11.5 cannot be extended to less basic pH values, for which the gel properties appear to differ. The data obtained at pH 7 and pH 8 show that silicon retention in the gel is considerably greater than at pH 9.5–11.5 (90% at pH 7 and 85% at pH 8, versus about 40% at pH > 9.5) and yet, the gels formed under these conditions are considerably less protective: the alteration rate diminishes to a much smaller extent at these pH values than for pH > 9.5 (Fig. 7). The silicon fraction retained in the gel is, thus, not the only parameter involved in the protective gel effect, and the condensation mechanism responsible for the gel formation is appreciably modified by the pH. Further data concerning the gel structure must be available before proceeding with the interpretation of the results.

In view of these arguments, it would appear more reasonable today to consider the steady-state concentration of dissolved Si as a consequence of the glass dissolution decrease, rather than a true equilibrium. This new interpretation could lead us to revise the expression of the glass dissolution kinetic laws.

4.5. Possibility of renewed alteration at pH < 10.8

Morphological and chemical examination of the surface of the glass powder grains altered at pH 11.5 revealed an outer region of secondary phases and an inner layer characteristic of the alteration gel. The EDS maps clearly show the heterogeneous aluminum distribution within the glass alteration products: Al tends to accumulate in the $Alc_2Al_2Si_4O_{12}$ crystals that the develop around the periphery of the alteration film. The aluminum balance shows that this element comes mainly from the gel. This is an important point, as it suggests that the precipitation of the $Alc_2Al_2Si_4O_{12}$ phase is directly related to the renewal of glass alteration. The most likely scenario to account for the glass behavior at pH 11.5 is the following.

1. A protective gel forms during the first few days of the experiment, causing the glass alteration rate to diminish sharply from the initial rate r_0 (Fig. 7). The aluminum is strongly incorporated in the gel, despite its high pH-dependent solubility.
2. The high solubility of Al ($32\ mg^{-1}$) and Si ($740\ mg\ l^{-1}$) after 56 days at pH 11.5 lead to the nucleation of $Alc_2Al_2Si_4O_{12}$ of crystals at the gel/solution interface.
3. The growth of these crystals consumes the dissolved Al and Si, and then the Al from the gel.
4. The dissolution of the Al in the gel and its precipitation in the $Alc_2Al_2Si_4O_{12}$ crystals cause the gel to lose its protective properties, resulting in a significant renewal of glass alteration.
5. When all the aluminum from the gel has been consumed, dissolution of the glass supplies Al directly to the $Alc_2Al_2Si_4O_{12}$ crystals.

The above process results in the complete transformation of the glass powder into alteration products without the formation of a new protective gel layer (Fig. 3).

This scenario establishes a causal relation between the precipitation of the $Alc_2Al_2Si_4O_{12}$ phase and the renewal of glass alteration. What then might be the limiting mechanism in this process, and what is the occurrence probability of such a phenomenon at less basic pH values? This is an essential question: the fact that the phenomenon was not observed below pH 11 does not exclude the possibility of its long-term occurrence. Renewed alteration occurred after 50 days at pH 11.5 and 250 days at pH 11. A purely kinetic limitation therefore cannot be ruled out.

The phase identified by XRD is not listed in the thermodynamic database. However, herschelite ($Si_2Al(Na,K)O_6,3H_2O$) is a known mineral that is observed during the alteration of some low- and intermediate-level nuclear glasses [26], and its composition is similar to that of the phase that precipitated in our experiment. The dissolution reaction for herschelite is

$$\begin{aligned} &Na_{0.5}L_{0.5}ALSi_{2.0}O_6,3H_2O\ (\text{solid}) + 4H^+\ (\text{aq}) \\ &\quad = 0.5Na^+(\text{aq}) + 0.5K^+(\text{aq}) + Al^{3+}(\text{aq}) \\ &\qquad + 2Si(OH)_4^0(\text{aq}) + H_2O. \end{aligned} \tag{15}$$

Log K was estimated at 7 for this reaction 90°C [27]. The saturation index was calculated for the glass alteration solution in all the experiments of this study (Fig. 18). The saturation index I_s is equal to log (Q/K), where Q is the ion activity product. The evolution of the leachate saturation index for herschelite versus the pH shows that the solutions in all the tests were largely oversaturated with respect to this mineral. Herschelite precipitation is thus, thermodynamically possible even at pH 7. The fact that none was observed at this pH (and the fact that it has never been observed in experiments with SON 68 glass at pH < 10), therefore, cannot be explained by thermodynamic constraints.

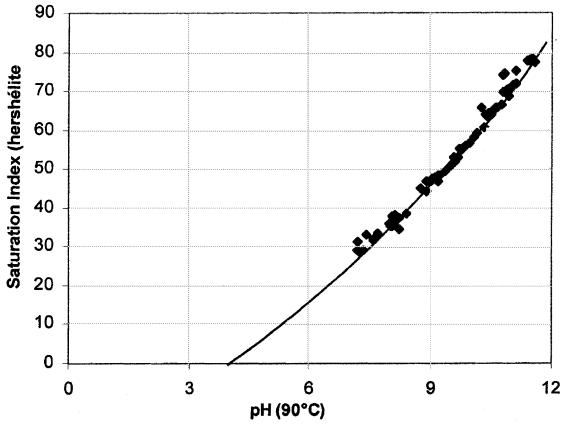

Fig. 18. Herschelite saturation index (LogQ/K) calculated from the chemical composition of the glass alteration solutions (data points for pH 7 to pH 11.5).

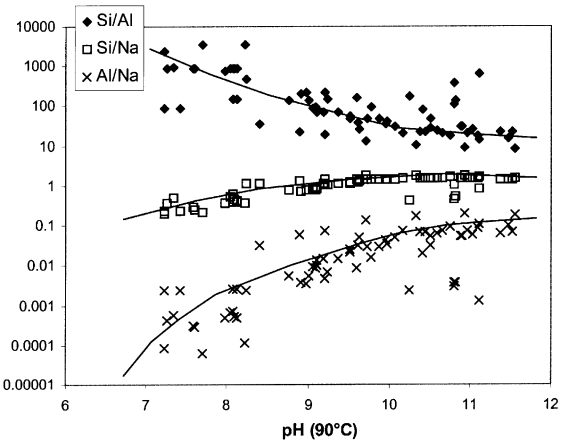

Fig. 19. Molar ratios of the main constituents of the $Alc_2Al_2Si_4O_{12}$ phase calculated from the glass alteration solution analysis results, showing a major Al deficit with respect to the $Alc_2Al_2Si_4O_{12}$ phase.

Fig. 19 shows the variation of the molar ratios of the dissolved species Si/Al, Si/Na and Al/Na versus the solution pH. The Si/Al and Si/Na ratios are both 2:1 in the $Alc_2Al_2Si_4O_{12}$ phase and the Al/Na ratio is 1:1 (assuming Alc = Na). Fig. 14 shows that above pH 9 the Si/Na ratio in solution is close to the ratio in the $Alc_2Al_2Si_4O_{12}$ phase. The Si/Al and Al/Na ratios, however, are far from the solid-phase values even at very basis pH levels. At pH 11.5, the Si/Al ratio in solution is 10 times higher than in the solid, whereas, the Al/Na ratio is 15 times lower. These differences increase as the pH diminishes. If precipitation of the $Alc_2Al_2Si_4O_{12}$ phase is assumed to be initiated by the solution – which would appear to be the case since no crystals are observed in the gel – then the limiting parameter appears to be the dissolved aluminum concentration in solution. The fact that the aluminium solubility is low, particularly at pH < 10, probably limits the number of crystals liable to precipitate. The crystal density above which growth occurs from the gel is unknown, but it is reasonable to assume that below pH 10 the Al deficit is sufficient to inhibit the process.

5. Conclusion

The pH appears to be a key parameter in the long-term behavior of SON 68-type nuclear glass because of its considerable influence on the glass alteration kinetics. In order to take this effect into account in a long-term behavior model, we must first understand how the pH modifies the protective properties of the gel and the apparent solubility of the glass.

This study has revealed the need for discriminating between the mechanisms above and below the glass equilibrium pH. The mechanisms of gel formation and

its protective properties are pH-independent below the glass equilibrium pH (about 9 at 90°C), but are pH-dependent above the equilibrium value. We have also shown that the gels formed at pH > 9 are more protective than those formed between pH 7 and pH 9.

We have established a dissolution/reprecipitation mechanism in highly basic media (pH > 11) resulting in the loss of the gel protective properties and renewed glass alteration leading to the complete transformation of the glass powder into alteration products. The $Alc_2Al_2Si_4O_{12}$ phase that precipitates consumes elements from the gel, notably aluminum. We have shown that the solubility of aluminum limits the development of this phase. Under these conditions, pH values below 10 should limit the onset and avoid the consequences of such precipitation. This crucial conclusion, which concerns the long-term durability of the gel, is supported by the results of an experiment in which a protective gel was perturbed by modifying the solution pH: we have shown that the glass does not react to an upward shift in the pH as long as it remains below 10. The pH-dependence of the apparent glass silica solubility differs from that of a pure silica phase, mainly because silicon is not the only kinetically limiting element. Moreover, although the development of highly protective gels leads to the establishment of quasi steady-state silicon concentrations in solution, we have shown (1) that these quasi steady-state conditions are only an approximation of reality, as the silicon concentrations increase slowly but steadily over time, and (2) that they depend on extrinsic factors such as the S/V ratio and, more generally, the protective properties of the gel – and thus, on the gel formation conditions. For these reasons, we have prudently referred to the 'apparent glass silicon solubility' to distinguish this phenomenon from the true thermodynamic solubility.

Acknowledgements

The authors are grateful to the reviews of this article, who notably suggested that another test be conducted a pH > 11 on a SON 68-type glass without aluminum to confirm the proposed mechanism.

References

[1] R.K. Iler, The Chemistry of Silica, Wiley, New York, 1979, p. 866.
[2] A.C. Lasaga, in: A.F. White, S.L. Brantley (Eds.), Chemical Weathering Rates of Silicates Minerals, Rev. Min. 31 (1995) 23.
[3] B. Grambow, Uhlig's Handbook, 2nd Ed., 2000, 411.
[4] P. Aagaard, H.C. Helgeson, Am. J. Sci. 282 (1982) 237.
[5] S. Gin, C. Jégou, Am. J. Sci. (2000) (submitted).
[6] C. Jégou, PhD thesis, Université de Montpellier II, 1998.
[7] S. Gin, C. Jégou C., E.J. Vernaz, F. Larché, in: International Conference on Glass XVIII, July, 1998, American Ceramic Society, Washington, DC, 1999.
[8] I. Técher, PhD thesis, Université de Montpellier II, 1999.
[9] S. Gin, C. Jegou, E.Y. Vernaz, Appl. Geochem. 15 (2000) 1505.
[10] S. Gin, P. Jollivet, J.P. Mestre, M. Jullien, C. Pozo, Appl. Geochem. (2000) (accepted).
[11] S. Gin, L. Ribet, M. Couillaud, J. Nucl. Mater., 2000 (to be published).
[12] C. Jégou, S. Gin, F. Larché, J. Nucl. Mater. 280 (2000) 216.
[13] T. Advocat, J.L. Crovisier, E.Y. Vernaz, G. Ehret, H. Charpentier, Mater. Res. Soc. Symp. Proc. 212 (1991) 57.
[14] Madé B. (1991), PhD thesis, Université Louis Pasteur, Strasbourg.
[15] B.E. Scheetz, W.P.D.K. Freeborn, C. Anderson, M. Zolensky, W.B. White, Mater. Res. Soc. Symp. Proc. 44 (1985) 129.
[16] T. Advocat, PhD thesis, Université Louis Pasteur, Strasbourg, 1991.
[17] J. Schwarzentruber, W. Furst, H. Renon, Geochim. Cosmochim. Acta 51 (1987) 1867.
[18] B. Grambow, Mater. Res. Soc. Symp. Proc. 44 (1985) 15.
[19] J. Caurel, PhD thesis, Université de Poitiers, 1990.
[20] Gin S. (unpublished data).
[21] Z. Boksay, G. Bouquet, S. Dobos, Physics Chem. Glasses 9 (1968) 69.
[22] H. Doremus, J. Non-Cryst. Solids 19 (1975) 137.
[23] B. Grambow, J. Nucl. Mater. (2000b) (to be published).
[24] S. Ricol, PhD thesis, Université Pierre et Marie Curie, 1995.
[25] E.Y. Vernaz, J.L. Dussossoy, Appl. Geochem. Suppl. (1) (1992) 13.
[26] B.P McGrail, D.H. Bacon, J.P. Icenhower, P.F. Martin, S.V. Mattigod, J. Nucl. Mater. (2000) (to be published).
[27] S.V. Mattigod, B.P. McGrail, Micropor. Mesopor. Mater. 27 (1999) 41.